Another suggestion for an interstellar C_5H_2 search[1]

S. Chandra [2], P. G. Musrif, S. V. Shinde and S. A. Shinde

School of Physical Sciences, S.R.T.M. University, Nanded 431 606, India

Abstract. Laboratory detection of four isomers of C_5H_2 molecule have been reported by Travers et al. [1], McCarthy et al. [2] and Gottlieb et al. [3]. Two transitions $3_{13} - 2_{12}$ and $3_{03} - 2_{02}$ at 19.147 GHz and 19.606 GHz, respectively, of c-C_5H_2 (isomer 1) have been detected in TMC-1 by Dickens et al. [4]. Chandra and Shinde [5] suggested that the c-C_5H_2 may be identified in cool cosmic objects through its transition $3_{13} - 4_{04}$ at 4.3 GHz in absorption against the cosmic microwave background. Here, we have investigated the third isomer of C_5H_2. A number of lines $4_{14} - 5_{05}$, $3_{13} - 4_{04}$, $2_{12} - 3_{03}$, $6_{15} - 6_{06}$ and $5_{14} - 5_{05}$ of the isomer have been found in absorption against the CMB. We propose that detection of $4_{14} - 5_{05}$ and $3_{13} - 4_{04}$ transitions at 4.8 GHz, 63.9 GHz, respectively of this isomer against CMB may be used for identification of C_5H_2. Since in absence of availability of the collisional rates, we have used scaled values for them, we have checked the sensitivity of the lines on the rates by enhancing the rates for the transitions with $\Delta k_a = 0$ by a factor of 10. The results are not found sensitive.

Key words. interstellar molecules - C_5H_2

1 Introduction

Out of the four isomers of C_5H_2 (Figure 1), two transitions $3_{13} - 2_{12}$ and $3_{03} - 2_{02}$ at 19.147 GHz and 19.606 GHz, respectively, of c-C_5H_2 (isomer 1) have been detected in TMC-1 by Dickens et al. [4]. Chandra and Shinde [5] suggested that detection of $3_{13} - 4_{04}$ transition of c-C_5H_2 at 4.314 GHz in absorption against the cosmic microwave background (CMB) may be used for identification of C_5H_2 in cool cosmic objects. Chandra et al. [6] have also suggested that the c-C_7H_2 (next molecule of the series c-C_3H_2, c-C_5H_2) may be identified in cool cosmic objects through its transitions $4_{14} - 5_{05}$, $5_{15} - 6_{06}$, $6_{16} - 7_{07}$ and $7_{17} - 8_{08}$ at 23.241 GHz, 21.105 GHz, 18.953 GHz and 16.787 GHz, respectively, in absorption against the CMB.

The third isomer of C_5H_2 molecule (Figure 1) is an asymmetric top, planar molecule having an electric dipole moment 4.8 Debye which is inclined with the axes of inertia so that its components along the a and b axes of inertia are $\mu_a = 2.84$ Debye and $\mu_b = 3.86$ Debye. Thus, this isomer has both a-type and b-type radiative transitions, and therefore, the rotational energy levels cannot be separated into two different groups. Hence, the investigation of this molecule also is quite complicated. The molecular data derived by Gottlieb et al. [3] for this isomer of C_5H_2 are given in Table 1. Since the kinetic temperature in dark molecular clouds is rather low, only rotational transitions in the ground electronic and ground vibrational states take place. A number of lines $4_{14} - 5_{05}$, $3_{13} - 4_{04}$, $2_{12} - 3_{03}$, $6_{15} - 6_{06}$ and $5_{14} - 5_{05}$ of the third isomer have been found in anomalous absorption. We propose here to identify this isomer of C_5H_2 in cool cosmic objects through the transitions $4_{14} - 5_{05}$ and $3_{13} - 4_{04}$ at 4.8 GHz and 63.9 GHz, respectively.

[1] Tables 3 is available only in the electronic form

[2] Visiting Associate of IUCAA, Pune 411 007, India ; Email: sch@iucaa.ernet.in

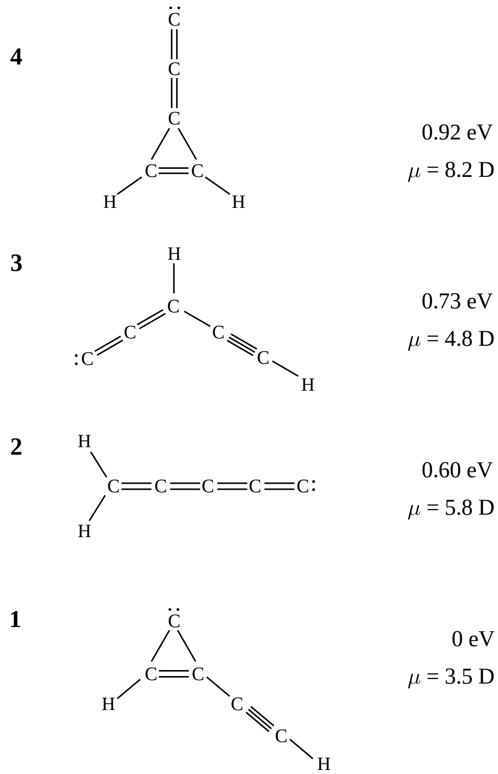

Figure 1: Structure of four isomers of C_5H_2 molecule along with electric dipole moment & their energy relative to isomer 1.

Table 1. Molecular Data for third isomer of C_5H_2

A (MHz)	318166
B (MHz)	2865.77293
C (MHz)	2624.47953
Δ_J (MHz)	1.4718x 10^{-3}
Δ_{JK} (MHz)	-0.13972
δ_J (MHz)	0.3716x 10^{-3}
μ_a (Debye)	2.84
μ_b (Debye)	3.86

2 Basic formulation

In our investigation, NLTE occupation numbers of the levels are calculated in an on-the-spot approximation by using the escape probability method [6], where the external radiation field, impinging on a volume element generating the lines, is the CMB only. In the present investigation, a set of 61 linear equations coupled with 309 equations of radiative transfer is solved through iterative procedure for the given values of n_{H_2} and $\gamma \equiv n_{\rm mol}/(dv_r/dr)$, where $n_{\rm mol}$ is density of the molecule and dv_r/dr the velocity gradient in the object. The input data required in the present investigation are the radiative transitions probabilities (Einstein A-coefficients) and the collisional rate coefficients.

3 Einstein A-coefficients

Rotational wave functions for an asymmetric top molecule can be described as linear combination of symmetric top wave functions [5]

$$\Psi_{J\tau M}(\alpha,\beta,\gamma) = \sqrt{\frac{2J+1}{8\pi^2}} \sum_{K=-J}^{J} g^J_{\tau K} D^J_{MK}(\alpha,\beta,\gamma)$$

where α, β, γ are Euler angles specifying the orientation of the molecule, J the rotational quantum number, $g^J_{\tau K}$ the expansion coefficients, D^J_{MK} the Wigner D-function and the pseudo quantum number τ is defined by

$$\tau = k_a - k_c$$

where k_a and k_c are projections of J on the axis of symmetry in case of prolate and oblate symmetric tops, respectively. Rotational levels in an asymmetric top molecule are specified as J_{k_a,k_c} or J_τ. The rotational energy levels accounted in the present investigation are given in Table 3. In the calculations, 9 pairs of levels having equal energies are combined.

Since the electric dipole moment of the molecule is inclined with its axes of inertia, it has both a-type as well as b-type radiative transitions. The a-type radiative transitions are governed by the selection rules

$$\begin{aligned} J: &\quad \Delta J = 0, \pm 1 \\ k_a, k_c: &\quad \text{even, odd} \longleftrightarrow \text{even, even} \\ &\quad \text{odd, even} \longleftrightarrow \text{odd, odd} \end{aligned}$$

In the representation where the axis of quantization is along the a-axis of inertia, Einstein A-coefficient for the transition $J'_{\tau'} \to J_\tau$ is [6]

$$A(J'_{\tau'} \to J_\tau) = \frac{64\pi^4\nu^3\mu_a^2(2J+1)}{3hc^3(2J'+1)} \Big[\sum_{K=-J}^{J} g^J_{\tau K} g^{J'}_{\tau' K} C^{J'K}_{JK10} \Big]^2$$

where μ_a is the electric dipole moment along the a-axis of inertia and $\mathbf{C}^{\cdot\cdot}_{\cdots\cdot}$ the Clebsch Gordon coefficient. The b-type rotational transitions are governed by the selection rules

$$\begin{aligned} J: &\quad \Delta J = 0, \pm 1 \\ k_a, k_c: &\quad \text{even, odd} \longleftrightarrow \text{odd, even} \\ &\quad \text{even, even} \longleftrightarrow \text{odd, odd} \end{aligned}$$

In the representation where the axis of quantization is along the a-axis of inertia, Einstein A-coefficient for the transition $J'_{\tau'} \to J_\tau$ is [6]

$$A(J'_{\tau'} \to J_\tau) = \frac{32\pi^4\nu^3\mu_b^2(2J+1)}{3hc^3(2J'+1)} \Big[\sum_{K=-J}^{J} g^J_{\tau K} \Big(g^{J'}_{\tau' K+1} C^{J'K+1}_{JK11} + g^{J'}_{\tau' K-1} C^{J'K-1}_{JK1,-1} \Big) \Big]^2$$

where μ_b is the electric dipole moment along the b-axis of inertia. Calculated values of the Einstein A-coefficients for a-type as well as b-type rotational transitions between the levels up to 18 cm^{-1} are available in the electronic form in Table 3.

Table 2. Energy levels of the isomer 3 of C_5H_2

J	k_a	k_c	$E(\mathrm{cm}^{-1})$	J	k_a	k_c	$E(\mathrm{cm}^{-1})$
0	0	0	0.000	1	0	1	0.183
2	0	2	0.549	3	0	3	1.099
1	1	1	1.149	1	1	0	1.157
2	1	2	1.507	2	1	1	1.531
4	0	4	1.831	3	1	3	2.044
3	1	2	2.093	5	0	5	2.745
4	1	4	2.761	4	1	3	2.841
5	1	5	3.656	5	1	4	3.777
6	0	6	3.842	2	2	1	4.428
2	2	0	4.428	6	1	6	4.730
6	1	5	4.899	3	2	2	4.978
3	2	1	4.978	7	0	7	5.121
4	2	3	5.710	4	2	3	5.711
7	1	7	5.984	7	1	6	6.209
8	0	8	6.582	5	2	4	6.626
5	2	3	6.628	8	1	8	7.415
8	1	7	7.705	6	2	5	7.725
6	2	4	7.728	9	0	9	8.224
7	2	6	9.007	7	2	5	9.013
9	1	9	9.026	9	1	8	9.388
3	3	1	9.827	3	3	0	9.827
10	0	10	10.047	8	2	7	10.471
8	2	6	10.482	4	3	2	10.560
4	3	1	10.560	10	1	10	10.815
10	1	9	11.257	5	3	3	11.476
5	3	2	11.476	11	0	11	12.051
9	2	8	12.119	9	2	7	12.135
6	3	4	12.575	6	3	3	12.575
11	1	11	12.783	11	1	10	13.313
7	3	5	13.858	7	3	4	13.858
10	2	9	13.949	10	2	8	13.974
8	3	6	15.324	8	3	5	15.325
11	2	10	15.962	11	2	9	15.998
9	3	7	16.974	9	3	6	16.974
4	4	1	17.348	4	4	0	17.348

4 Collisional rate coefficients

Besides the radiative transition probabilities for radiatively allowed transitions between the rotational energy levels, data required as input for the present investigation are the rate coefficients for collisional transitions between the levels due to collisions with H_2 molecules. Though the collisional transitions are not restricted through any selection rules, computation of them is a quite cumbersome task. These required collisional rate coefficients are not available in the literature. In absence of them, qualitative investigations can however be carried out by choosing some scaling laws for the rate coefficients which do not favour any anomalous behaviour from their own. As and when the collisional rate coefficients would be available, the investigation can be repeated for quantitative results. In the present investigation, the rate coefficients for downward transitions $J'k_a'k_c' \to Jk_ak_c$ at a kinetic temperature T are taken as [7]

$$C(J'k_a'k_c' \to Jk_ak_c) = \frac{1\mathrm{x}10^{-11}}{(2J'+1)} \sqrt{\frac{T}{30}}$$

These rate coefficients can be interpreted as the cross section times a thermal velocity. The factor $(2J'+1)$ is the degeneracy of the upper level of the transition. These rates have no selectivity and do not support any anomalous behaviour from their own. However, some transitions between the low lying levels may be sensitive to the collisional rates.

In order to check the sensitivity of our results to the collisional rates, we enhanced the collisional rates for the transitions with $\Delta k_a = 0$ by a factor of 10 (i.e., by one order of magnitude), which may be taken as an extreme case. The results with these enhanced rates are also given in this paper (column 4 in Figures 2 and 3). Moreover, in absence of the accurate collisional rates, our results can be treated as qualitative in nature.

For upward collisional rate coefficients, we accounted for the fact that downward and upward collisional rate coefficients are related through the detailed equilibrium [8].

5 Anomalous absorption

Observation of a spectral line in absorption against the CMB is an unusual phenomenon. The intensity, I_ν, of a line generated in an interstellar cloud, with homogeneous excitation conditions, is given by

$$I_\nu - I_{\nu,bg} = (S_\nu - I_{\nu,bg})(1 - e^{-\tau_\nu}) \quad (1)$$

where $I_{\nu,bg}$ is the intensity of the continuum against which the line is observed, τ_ν the optical depth of the line and S_ν the source function. For positive optical depth, observation of an interstellar line in absorption against the CMB (i.e., $I_\nu < I_{\nu,bg}$), obviously, implies the excitation temperature T_{ex} of the line to be less than the CMB-temperature T_{bg}, but positive ($0 < T_{ex} < T_{bg}$). It requires rather peculiar conditions in the molecule generating the line. Equation (1) may also be expressed as

$$B_\nu(T_B) - B_\nu(T_{bg}) = [B_\nu(T_{ex}) - B_\nu(T_{bg})](1 - e^{-\tau_\nu}) \tag{2}$$

where B_ν represents a Planck's function corresponding to various temperatures and T_B is the brightness temperature of the line. (For absorption against the CMB, we have ($T_B < T_{bg}$). This obviously shows that for optically thin case, $\tau_\nu \approx 0$ and we have $T_B = T_{bg} \equiv 2.7$ K. Further, in the Rayleigh-Jeans limit [ν(GHz) $<< 21\ T$(K)], Equation (2) can be written as

$$T_B = T_{ex} + (T_{bg} - T_{ex})e^{-\tau_\nu} \tag{3}$$

For anomalous absorption, we have $T_{ex} < T_{bg}$ and $\tau_\nu > 0$, and therefore, $T_B > T_{ex}$. When τ_ν is very large, then for the anomalous absorption, we have $T_B = T_{ex}$. It shows that for anomalous absorption, the brightness temperature of the line lies between T_{ex} of the line and T_{bg} ($T_{ex} \le T_B \le T_{bg}$).

6 Numerical results and discussion

In our model, the free parametres are the hydrogen density n_{H_2} and γ. In order to include a large number of cosmic objects where C_5H_2 may be found, numerical calculations are carried out for wide ranges of physical parametres. In our earlier work [5] for c-C_5H_2 (isomer 1), we had taken $\gamma = 10^{-5}$ cm^{-3} (km/s)$^{-1}$ pc and 10^{-4} cm^{-3} (km/s)$^{-1}$ pc. These values are taken here for third isomer of C_5H_2 also. The molecular hydrogen density n_{H_2} is varied over the range from 10^3 to 10^6 cm^{-3}, and calculations are performed for two kinetic temperatures 10 and 15 K, as the temperature in a cool cosmic object would be around that.

A number of lines of the third isomer of C_5H_2 are found in absorption against the CMB. However, the transitions $4_{14} - 5_{05}$, $3_{13} - 4_{04}$, $2_{12} - 3_{03}$, $6_{15} - 6_{06}$ and $5_{14} - 5_{05}$ have shown good absorption phenomenon. For these transitions, we have plotted T_B (column 1), T_{ex} (column 2), τ_ν (column 3) and again T_B (column 4) where the enhanced collisional rates are used.

Figure 2 and 3 shows that the transitions $4_{14} - 5_{05}$ and $3_{13} - 4_{04}$ may be used for identification of the molecule through anomalous absorption phenomenon. With the increase in temperature, the position in the peak of brightness temperature is found to shift towards the low density region and the value of brightness temperature is found to decrease. The position in the peak of optical depth is also found to shift towards the low density region and the optical depth increases. Moreover, the identification of C_5H_2 may be hampered due to its low column density. Since, we have used scaled values of collisional rates and therefore, our results are qualitative in nature.

7 Acknowledgements

We are grateful to Prof. Jayant V. Narlikar, Prof. Dr. W.H. Kegel and for their encouragement. Thanks are due to Mr. Ram M. Dharmkare for helpful discussion.

References

[1] M.J. Travers, M.C. McCarthy, C.A. Gottlieb, P. Thaddeus, *ApJ* **483** (1997), L135.

[2] M.C. McCarthy, M.J. Travers, A. Kovacs, W. Chen, S.E. Novick, C. A. Gottlieb, P. Thaddeus, *Science* **275** (1997) 518.

[3] C.A. Gottlieb, M.C. McCarthy, V.D. Gordon, J.M. Chakan, A.J. Apponi, P. Thaddeus, *ApJ* **509** (1998) L141.

[4] J.E. Dickens, W.D. Langer, T. Velusamy, *ApJ* **558** (2001) 693.

[5] S. Chandra, S.A. Shinde, *A&AS* **423** (2004) 325.

[6] S. Chandra, P.G. Musrif, R.M. Dharmkare, *New Astronomy* **10** (2005)385.

[7] A. K. Sharma, S. Chandra, *A&AS* **376** (2001) 333.

[8] S. Chandra, W.H. Kegel, *A&AS* **142** (2000) 113.

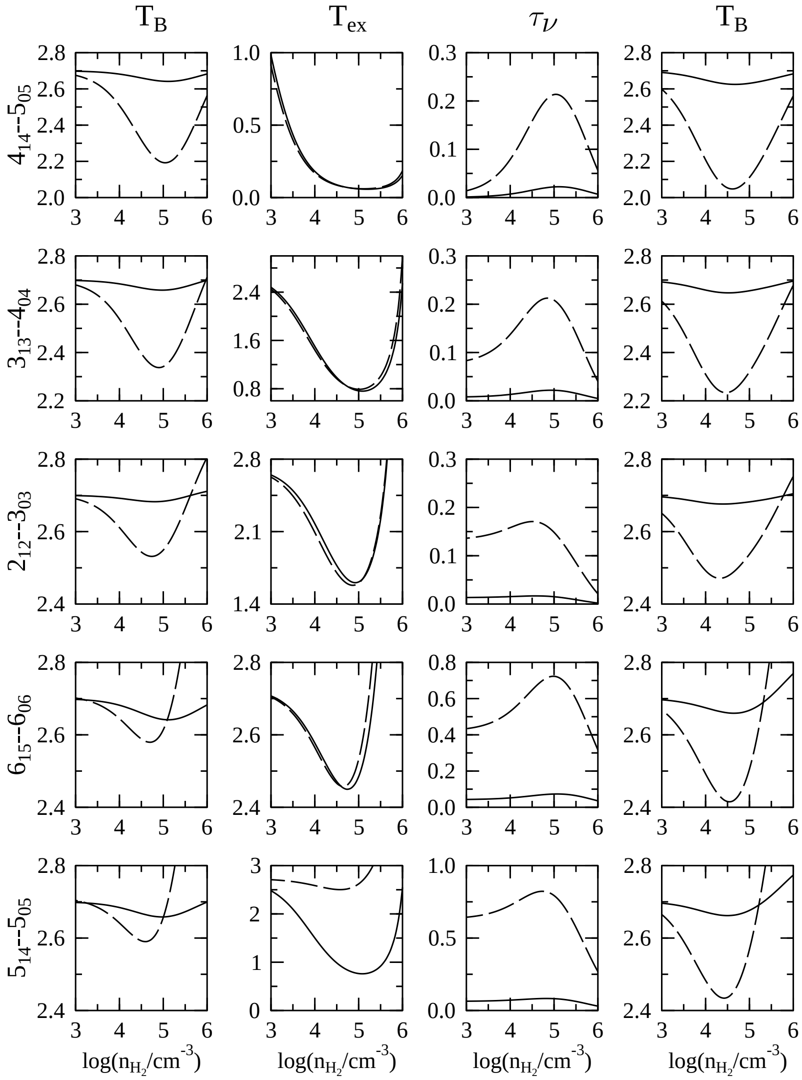

Figure 2: Variation of brightness temperature T_B (K) (column 1), excitation temperature T_{ex} (K) (column 2), optical depth τ_ν (column 3) versus hydrogen density n_{H_2} for kinetic temperature of 10 K for the transitions written on the left. Solid line is for $\gamma = 10^{-5}$ cm^{-3} (km/s)$^{-1}$ pc, and the dotted line for $\gamma = 10^{-4}$ cm^{-3} (km/s)$^{-1}$ pc. For thebrightness temperature T_B in column 4, the collisional rates for the transitions with $\Delta k_a = 0$ are increased by a factor of 10. Comparison of columns 1 and 4 shows that the results are not sensitive to the collisional rates.

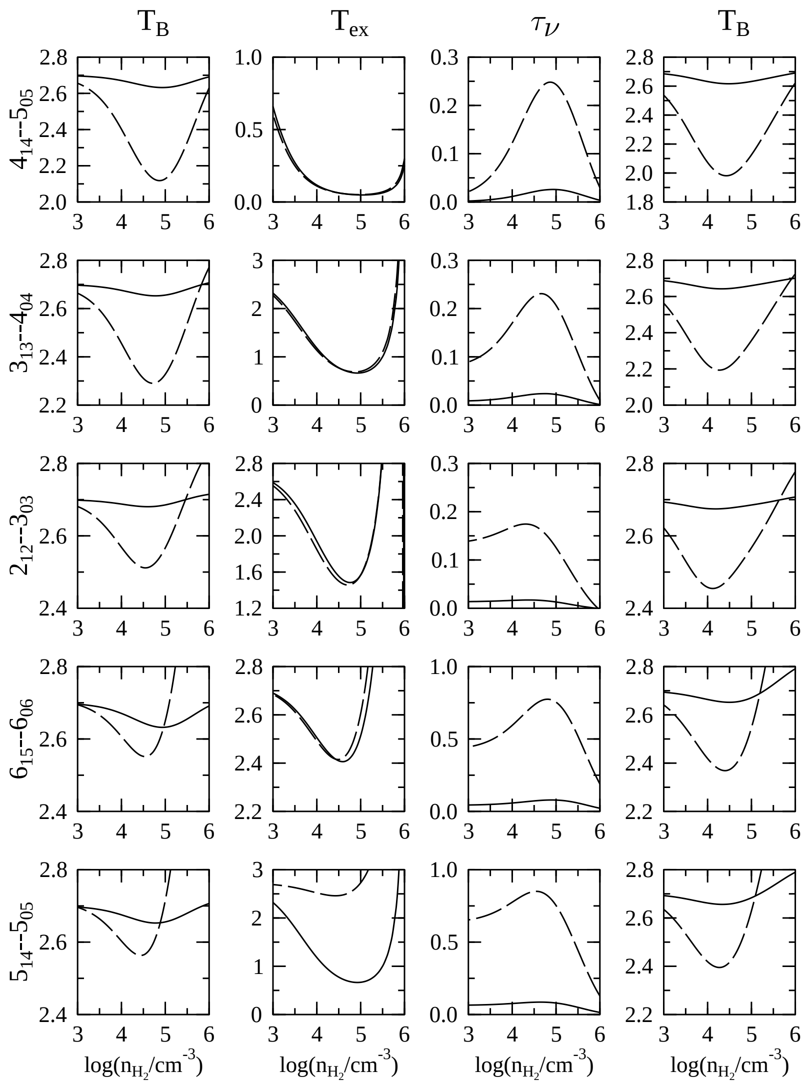

Figure 3: Variation of brightness temperature T_B (K) (column 1), excitation temperature T_{ex} (K) (column 2), optical depth τ_ν (column 3) versus hydrogen density n_{H_2} for kinetic temperature of 15 K for the transitions written on the left. Solid line is for $\gamma = 10^{-5}$ cm^{-3} (km/s)$^{-1}$ pc, and the dotted line for $\gamma = 10^{-4}$ cm^{-3} (km/s)$^{-1}$ pc. For thebrightness temperature T_B in column 4, the collisional rates for the transitions with $\Delta k_a = 0$ are increased by a factor of 10. Comparison of columns 1 and 4 shows that the results are not sensitive to the collisional rates.